Clinical Neurophysiology 120 (2009) 1262–1272

Contents lists available at ScienceDirect

Clinical Neurophysiology

journal homepage: www.elsevier.com/locate/clinph

Removing muscle and eye artifacts using blind source separation techniques in ictal EEG source imaging

H. Hallez [a,*], M. De Vos [b], B. Vanrumste [b], P. Van Hese [a], S. Assecondi [a], K. Van Laere [d], P. Dupont [e], W. Van Paesschen [c], S. Van Huffel [b], I. Lemahieu [a]

[a] Department of Electronics and Information Systems, MEDISIP – IBBT-IBITECH, Ghent University, De Pintelaan 185, 9000 Ghent, Belgium
[b] Department of Electrical Engineering (ESAT), SCD-SISTA, K.U. Leuven, Kasteelpark Arenberg 10, Leuven, Belgium
[c] Department of Neurology, Division of Experimental Neurology, University Hospital Gasthuisberg, Herestraat 49, 3000 Leuven, Belgium
[d] Department of Medical Diagnostic Sciences, Division of Nuclear Medicine, University Hospital Gasthuisberg, E901, Herestraat 49, 3000 Leuven, Belgium
[e] Department of Neurosciences, Laboratory for Cognitive Neurology, K.U. Leuven, Herestraat 49, 3000 Leuven, Belgium

ARTICLE INFO

Article history:
Accepted 2 May 2009
Available online 17 June 2009

Keywords:
Ictal SPECT
Artifact removal
EEG source localization

ABSTRACT

Objective: The contamination of muscle and eye artifacts during an ictal period of the EEG significantly distorts source estimation algorithms. Recent blind source separation (BSS) techniques based on canonical correlation (BSS-CCA) and independent component analysis with spatial constraints (SCICA) have shown much promise in the removal of these artifacts. In this study we want to use BSS-CCA and SCICA as a preprocessing step before the source estimation during the ictal period.
Methods: Both the contaminated and cleaned ictal EEG were subjected to the RAP-MUSIC algorithm. This is a multiple dipole source estimation technique based on the separation of the EEG in signal and noise subspace. The source estimates were compared with the subtracted ictal SPECT (iSPECT) coregistered to magnetic resonance imaging (SISCOM) by means of the euclidean distance between the iSPECT activations and the dipole location estimates. SISCOM results in an image denoting the ictal onset zone with a propagation.
Results: We applied the artifact removal and the source estimation on 8 patients. Qualitatively, we can see that 5 out of 8 patients show an improvement of the dipoles. The dipoles are nearer to or have tighter clusters near the iSPECT activation. From the median of the distance measure, we could appreciate that 5 out of 8 patients show improvement.
Conclusions: The results show that BSS-CCA and SCICA can be applied to remove artifacts, but the results should be interpreted with care. The results of the source estimation can be misleading due to excessive noise or modeling errors. Therefore, the accuracy of the source estimation can be increased by preprocessing the ictal EEG segment by BSS-CCA and SCICA.
Significance: This is a pilot study where EEG source localization in the presurgical evaluation can be made more reliable, if preprocessing techniques such as BSS-CCA and SCICA are used prior to EEG source analysis on ictal episodes.
© 2009 International Federation of Clinical Neurophysiology. Published by Elsevier Ireland Ltd. All rights reserved.

1. Introduction

Epilepsy is a neurological disorder caused by abnormal electrical activity of groups of neurons. The manifestion of such activity is called an epileptic seizure. Often, the disorder can be treated with medication. However, 30% of the patients develop drug-resistant epilepsy. These patients can sometimes be helped by resecting the origin of the epileptic seizure (the so-called epileptogenic focus) with a surgical operation. A presurgical evaluation has to be performed in order to determine an accurate location of the epileptogenic focus.

In the last decade different methods have been developed to estimate the location of the intracranial source of the epileptic activity from the scalp-EEG. Dipole models are used very often to represent focal epileptic activity. Dipolar models can be characterized by three spatial coordinates and three components, which have to be estimated by EEG dipole analysis (Baillet et al., 2001). It has been shown that the EEG dipole source analysis is a useful tool in the presurgical evaluation in ictal EEG (Boon et al., 2002) as well as inter-ictal EEG (Ding et al., 2006).

Another useful technique used in the presurgical evaluation to determine the ictal onset zone is SISCOM (subtracted ictal SPECT

* Corresponding author. Tel.: +32 93324326.
E-mail address: hans.hallez@UGent.be (H. Hallez).

1388-2457/$36.00 © 2009 International Federation of Clinical Neurophysiology. Published by Elsevier Ireland Ltd. All rights reserved.
doi:10.1016/j.clinph.2009.05.010

coregistered on MRI) (Van Paesschen et al., 2007; O'Brien et al., 1998). Specifically, single photon emission computed tomography (SPECT) provides a 3D distribution of the activity in the brain. In clinical practice, this technique can be used to image the location of the epileptogenic focus in the case of focal epilepsy.

Both techniques have benefits and drawbacks. The time resolution of the perfusion SPECT is in the order of 30–60 s and thus very low. In contrast, the EEG is a direct reflection of the electrophysiological activity, which results in a high temporal resolution (order of milliseconds). Regarding spatial resolution, SPECT (5–10 mm) outperforms EEG source estimation (2–4 cm according to Plummer et al. (2008)). Muscle activity and eye blink artifacts are two contributors to the distortions in the ictal EEG.

During a tonic or tonic–clonic epileptic seizure, muscle activity is very prominent and is reflected in the EEG by a high frequency random signal (Vergult et al., 2007). Localizing the source during an episode with muscle activity will most likely result in a source close to the muscles. Assaf and Ebersole (1997) used a very narrow bandpass filters (between 2 and 20 Hz) to remove the muscle and movement artifacts in spikes in order to obtain a signal with high signal-to-noise ratio. They showed that the source estimation correlated well with the temporal seizure onset zone. However, it is well known that the ictal EEG has a frequency of 0.5 between 45 Hz. Hence, the application of narrow band filters will filter out valuable information from the EEG (Goncharova et al., 2003).

Eye blink and eye movement artifacts are other sources of non-cerebral activity which can distort the EEG. These artifacts are caused by respectively closing/opening of the eyes and turning of the eye ball and are most prominent onto the EEG recorded from the electrodes placed near the eyes. The characteristics are low frequency content, non-stationarity and high amplitude (Niedermeyer and Lopez Da Silva, 2004).

Blind source separation (BSS) techniques have shown promising results in the field of artifact removal (Jung et al., 2000). De Clercq et al. used a BSS technique based on canonical correlation analysis (CCA), which assumes mutually uncorrelated sources which are maximally autocorrelated. Muscle sources indeed have a low autocorrelation with respect to brain activity (De Clercq et al., 2006). For the removal of eye-artifacts several techniques have been proposed. However, most of them require the availability of periocular electro-oculographic (EOG) electrodes (Shoker et al., 2005). These EOG electrodes are not always recorded as they are too cumbersome for the patient. Recently De Vos et al. (2006a) developed a spatially constrained ICA technique (SCICA) to remove eye blinks and movements. However, the feasibility of using these techniques to preprocess noisy EEG data prior to EEG source estimation is still unknown.

In this study we applied BSS-CCA (De Clercq et al., 2006) and SCICA (De Vos et al., 2006a) as a preprocessing step to remove artifacts for source analysis of EEG, contaminated with muscle and eye movement artifacts. In this way, we want to investigate qualitatively whether source localization of ictal EEG segments would benefit from artifact removal.

2. Materials

The EEG was measured in a clinical setup at the University hospital U.Z. Gasthuisberg in Leuven, Belgium. The electrodes were placed in a 10–20 standard system with 2 extra temporal electrodes and the sample rate was 250 Hz. From 8 patients where the SISCOM was concordant with other data of the presurgical evaluation (ictal semiology, interictal and ictal EEG, MRI, neuropsychological assessment) and was considered to reveal correctly the epileptogenic focus, the EEG was collected. The EEG segments were about 2 min in length and the start of the seizure was indicated by an experienced neurologist. Information about the patients used in this study is shown in Table 1. About 4 of 8 patients underwent a surgical procedure. One patient was rendered almost seizure free (Engel outcome II) and 3 patients were rendered seizure free completely (Engel outcome I).

3. Methods

3.1. Removing muscle and eye movement artifacts by blind source separation (BSS) techniques

The electroencephalogram (EEG) measures the sum of all electrical activity, synchronous neuronal firing and electrical artifacts. As these artifacts disturb accurate localization, they have to be removed first. The goal of independent component analysis (ICA) is to extract the source signals from a linear mixture of independent sources.

Mathematically, assume the basic linear statistical model

$$Y = \mathbf{M} \cdot X + N \tag{1}$$

where $Y \in \mathbb{R}^I$ is called the observation vector (I is the number of observation channels), $X \in \mathbb{R}^J$ the source vector (J is the number of sources) and $N \in \mathbb{R}^I$ additive noise. $\mathbf{M} \in \mathbb{R}^{I \times J}$ is the mixing matrix.

The goal of ICA is to estimate the mixing matrix $\mathbf{M}$, and/or the source vector X, given only realizations of Y. In this study, we assume that $I \geqslant J$.

Blind identification of $\mathbf{M}$ in (1) is only possible when some assumptions about the sources are made.

One assumption is that the sources are mutually statistically independent, as well as independent from the noise components and that at most one source is gaussian (Comon, 1994).

Table 1
The patient data used in the study. Gender: M, male; F, female; Frequency CPS, frequency of complex partial seizures per month; MRI: HS, hippocampal sclerosis; Nl, normal; CD, cortical dysplasia; PS, posttraumatic scar; EEG localization and SISCOM: L, left; R, right; T, temporal; F, frontal; C, central; O, occipital; NA, not applicable. Engel outcome scores: I, seizure free; II, almost seizure free; III, 75% seizure reduction; IV, no improvement. Duration of seizure is in seconds and time of injection is in seconds after the seizure onset.

Patient	Age	Gender	Age at onset	FrCPS	MRI	Lateralization	Ictal EEG	Duration of seizure (s)	Time of injection (s)	SISCOM	Surgery performed	Engel outcome
1	36	F	15	4	Nl	L	LFT	33	17	LT	No	NA
2	20	F	2	30	Nl	L	NA	93	25	LP	No	NA
3	35	F	25	15	HS	L	LT	94	12	LT	Yes	I
4	32	M	4	5	HS	L	LT	67	27	LT	Yes	I
5	30	M	6	8	CD	L	FC	70	18	LF	Yes	I
6	59	M	39	20	Nl	R	RT	96	17	RT	Yes	II
7	38	F	5	4	PS	L	LFC	36	3	LFT	No	NA
8	41	F	20	10	Nl	R	O	160	26	O	No	NA

An alternative assumption is that the sources are mutually uncorrelated but individually correlated in time. Under these assumptions, the sources can be estimated with the SOBI algorithm (Belouchrani et al., 1997). This algorithm has shown to be useful in several biomedical applications. The SOBI algorithm is based on second order statistics. This reduces the need for having long measurements of the observation signal as it is the case when higher order statistics are computed before computing the source signals (e.g. in Comon (1994)). This is necessary for the on-line application under investigation.

Due to the low frequency component, eye artifacts are highly autocorrelated in time and can be separated with SOBI from background EEG. With the standard SOBI algorithm, the sources corresponding to eye artifacts have to be selected after the decomposition. However, the spatial distributions of eye blink and eye movement artifacts are known from previous decompositions of EEG data. This prior knowledge can be exploited already during the computation of the individual independent sources. The artifactual source can be in this way automatically removed from the EEG measurements. This algorithm is known as SCICA (De Vos, 2009; De Vos et al., 2006b; De Vos et al., 2006a), based on SOBI (Belouchrani et al., 1998), and more computational details can be found in the Supplementary Appendix A. This prior knowledge should not be individualied for different subjects as the algorithm does not use fixed constraints.

Yet another possible assumption in blind source separation is that the sources are individually correlated in time and that all sources have a different autocorrelation. In this case an algorithm based on Canonical correlation analysis (CCA) can be used to recover the source signals (Hotelling, 1936). Muscle artifacts are characterized by a much lower autocorrelation than background EEG. So CCA can be used to separate EEG containing muscle artifacts into sources with high autocorrelation, related to brain activity and sources with lower autocorrelation, related to artifacts (De Clercq et al., 2006). The artifactual sources are visually selected by means of a home-made graphical user interface (based on low autocorrelation) and subtracted from the EEG. More mathematical details about CCA can be found in the Supplementary Appendix B.

3.2. Estimating the sources by RAP-MUSIC

When the muscle and eye artifacts are removed, one can search for the dipole sources. The EEG dipole localization problem is twofold. First, the forward problem states the relations between the potential values at the scalp electrodes and a given source. The electrode potentials are obtained by solving the Poisson's equation given a dipole source in a specified geometry. The head model we used, was a realistic head model derived from an T1 magnetic resonance (MR) image. As an individual T1 MR image was not available, we used the same MR image to construct a head model for all patients. We used SPM to perform a segmentation on the anatomical T1 MR images (Friston, 2006). The head model was segmented in four compartments: scalp tissue, skull, cerebrospinal fluid (CSF) and brain tissue. The forward problem was then solved by using a finite difference method (Hallez et al., 2005). The conductivities of the compartments were isotropic and were equal to 0.33 S/m, 0.020 S/m, 1 S/m and 0.33 S/m for scalp tissue, skull, CSF and brain tissue respectively (Gonçalves et al., 2003). The 21 electrode positions were set in a standard 10–20 system and were hence not adjusted to the patient specific positions.

Second, the inverse problem searches parameters of the dipole given the scalp potentials. A number of methods have been developed to estimate the dipole source, depending on the assumptions on the input EEG potentials. In this study we used a multidipolar estimation technique, i.e. RAP-MUSIC (Mosher and Leahy, 1999). The method is explained more in detail in the Supplementary Appendix C. This technique divides the measurement space into two subspaces representing the signal and noise in the EEG. The signal subspace was derived from the EEG correlation matrix in the following way. A singular value decomposition was performed in each window. The signal subspace was constructed from the columns of the left-singular vectors, which are ordered according to the singular values. These singular values indicate the explained variance. Hence, the number of columns of the left-singular vectors was chosen so that the cumulative explained variance was 90% with a limit to five columns. The dimension of the signal subspace was thus variable over the time windows. Then a search grid of 10 mm resolution over the brain compartment is defined and a scanning procedure is performed. The position in the search grid whose forward solution has a maximal correlation with the signal subspace is chosen as a starting point to maximize the correlation with the signal subspace using a direct optimization of equation (C.2) by means of the Nelder–Mead simplex method. After the optimal position is found, its forward solution is projected away from the signal subspace and the procedure is repeated iteratively for the next dipole source.

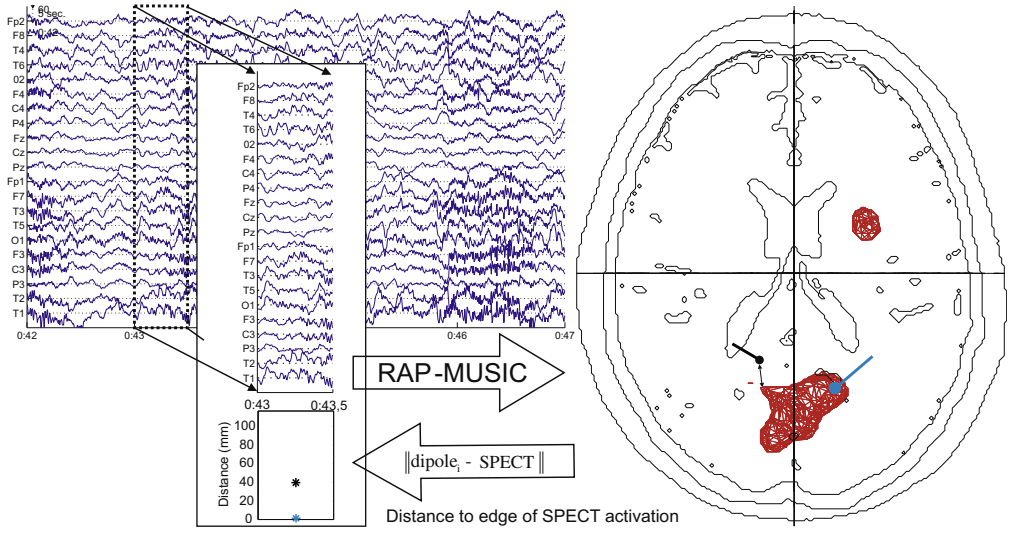


Fig. 1. A schematic of the calculation of the distance between the dipole locations and the edge of the 95% surface of the ictal SPECT activation. In a moving window of 62 samples (≈0.2 s) a maximum of two dipoles are estimated using the RAP-MUSIC algorithm. The distance of each dipole to the edge of the 95% interval of the ictal SPECT activation is then calculated and put in a separate figure.

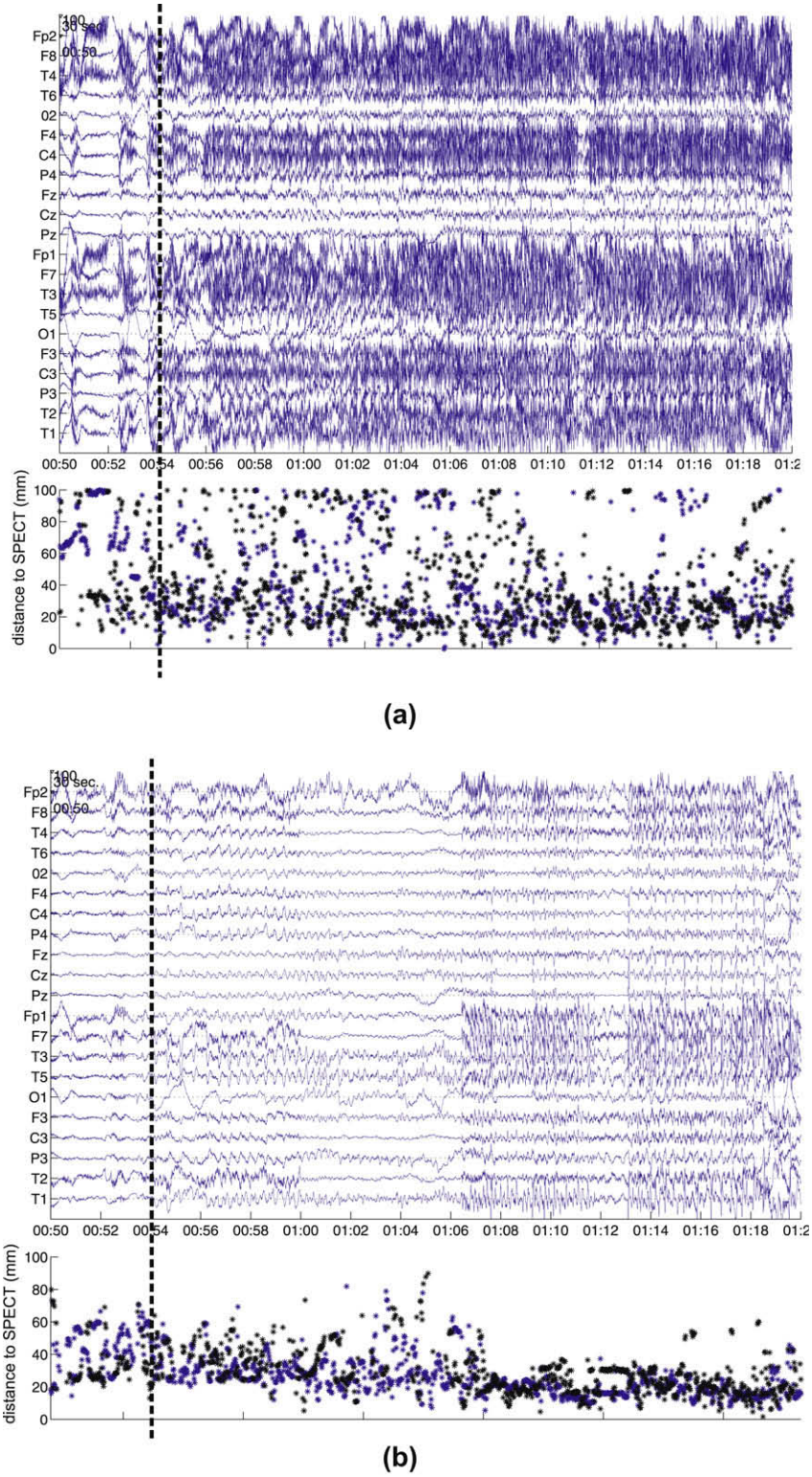


Fig. 2. In this figure we can see an EEG segment of 30 s in (a) the unfiltered case and (b) the filtered case. Below the EEG fragments the distance measure (in mm) is shown. The seizure start, as indicated by the neurologist, was between 53 and 54 s. In the unfiltered EEG, we can see that the distance from the dipole to the ictal SPECT activation is very high ($\geqslant$100 mm) and is very spread. The black asterisks and blue asterisks indicate the distance of the first and second dipole to the ictal SPECT activation, respectively. (For interpretation of color mentioned in this figure the reader is referred to the web version of the article.)

RAP-MUSIC was applied in moving windows of 62 samples ($\sim$0.25 s) with a step size of 6 samples ($\sim$0.025 s). In each window a maximum of two moving dipole sources were estimated using the scanning procedure over the search grid. Furthermore, the correlation between the forward solution of the dipole sources and the signal subspace should be at least 95%. This yields sources that are dominant in the EEG. If one of the sources did not meet the requirements, only one dipole was estimated. In addition to the traditional RAP-MUSIC algorithm described in Mosher and Leahy (1999), we restricted the dipole

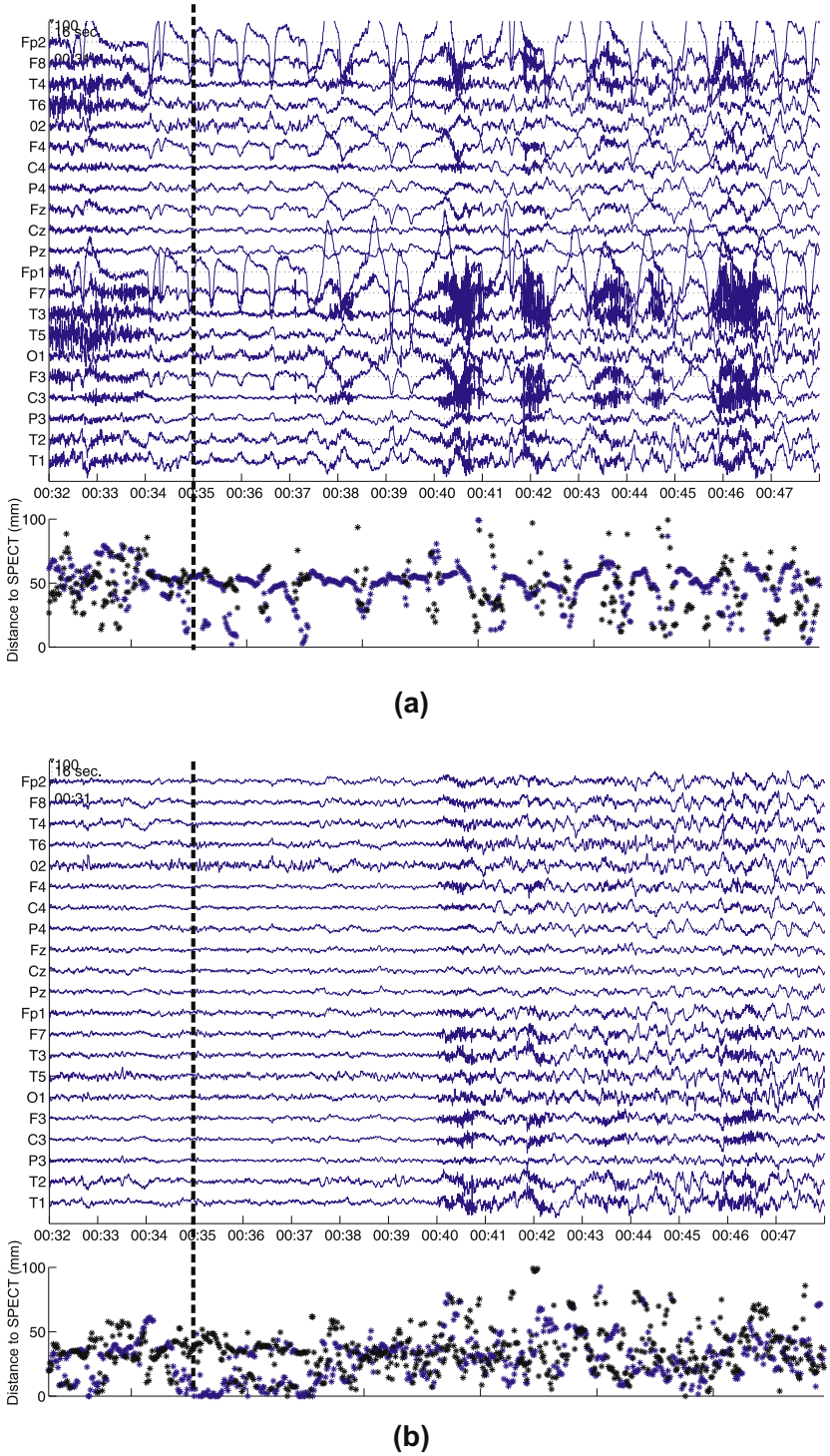


Fig. 3. (a) and (b) show the distance of the dipoles to the center of gravity of the ictal SPECT activation for the unfiltered and filtered EEG respectively in function of time. The results show an EEG window of 14 s and below the distance measure (in mm). The seizure start, as indicated by the neurologist, was at 35 s. In the unfiltered EEG, we can see that the distance from the dipole to the ictal SPECT activation is very high due to eye artifacts. In the filtered EEG, the dipoles from the early seizure onset are situated in or near the SPECT activation. The black asterisks and blue asterisks indicate the distance of the first and second dipole to the ictal SPECT activation, respectively. (For interpretation of color mentioned in this figure the reader is referred to the web version of the article.)

estimation in such way that the distance of the two dipole estimations was larger than 1 cm. The reason for this was that it sometimes occurred that the dipoles were modeling pure noise and tried to represent very low potentials at the electrodes. The result is that one obtains dipole estimations that have a high magnitude but cancel each other out.

When used in a moving window, *RRE* (see equation (C.3)) can be seen as an inverse goodness-of-fit in function of time. The lower the RRE, the better the dipoles represent the EEG segment. Hence, a lower RRE and thus a higher "goodness-of-fit" is a characterization of the focality of the sources. To identify focal sources, we selected the dipole estimations that resulted in an RRE within the first quartile of the total set of RREs in the 21 s time window: 1 s before till 20 s after the start of the seizure. In this way we selected the sources that gave the best goodness-of-fit of the dipole estimations. Hence, the goodness-

of-fit is dependent on each patient and on the noise in the EEG. Hence, in Hallez et al. (2007) it was shown that the RRE decreased when filtering the EEG. By choosing the first quartile we wanted to have an objective measure of the goodness-of-fit of the dipole estimations, as this takes into account the statistical distribution of the RRE over the whole 21 s time window.

3.3. Fusing the EEG dipole source estimations and SPECT activity

The SISCOM image is then coregistered to the MR image, from which the head model was made using SPM5 (Friston, 2006). The SPECT image of the SISCOM was normalized and a 95% threshold with respect to the maximum was set, considering only the activity above that threshold. We assumed that the edge of the 95% surface confined the seizure onset zone. Note that the activity delineated by the 95% surface could also be multifocal. In that case, the epileptic seizure was already propagated into other regions.

3.4. Experimental setup

Starting from the EEG segment of about two minutes of the 8 patients, the EEG was processed using the CCA and the SCICA algorithms to filter out the muscle and eye blink artifacts. The SCICA algorithm can be applied automatically as the topography of the eye blink artifacts is known. The muscle artifact removal by CCA is done semi-automatically as follows. An expert was presented with 10 s segments of EEG and using a graphical user interface the expert could increment or decrement the number of components removed from the presented segment. When the muscle artifact was removed, the expert continued to the next 10 s segment. For each patient we obtained a raw and a filtered EEG. Both the filtered and unfiltered EEG segments were processed by RAP-MUSIC as described above. The seizure onset on the EEG was depicted by a neurologist. The source estimations were done in moving windows from 1 s before the seizure onset to 20 s after the seizure onset. In this way we want to compensate for the difference in timing of the SPECT activation and the EEG dipole source estimations.

By combining the ictal SPECT activity with the dipole estimations from the RAP-MUSIC algorithm, we can evaluate the proximity of the dipole estimations before and after the artifact removal (see Fig. 1). The distances of the estimated dipoles with respect to the SPECT activations during the time period of 21 s were calculated. The result is a set of Euclidean distances for each of the at maximum two dipoles in that window. A boxcar plot is shown to compare the distributions of the distances before and after filtering.

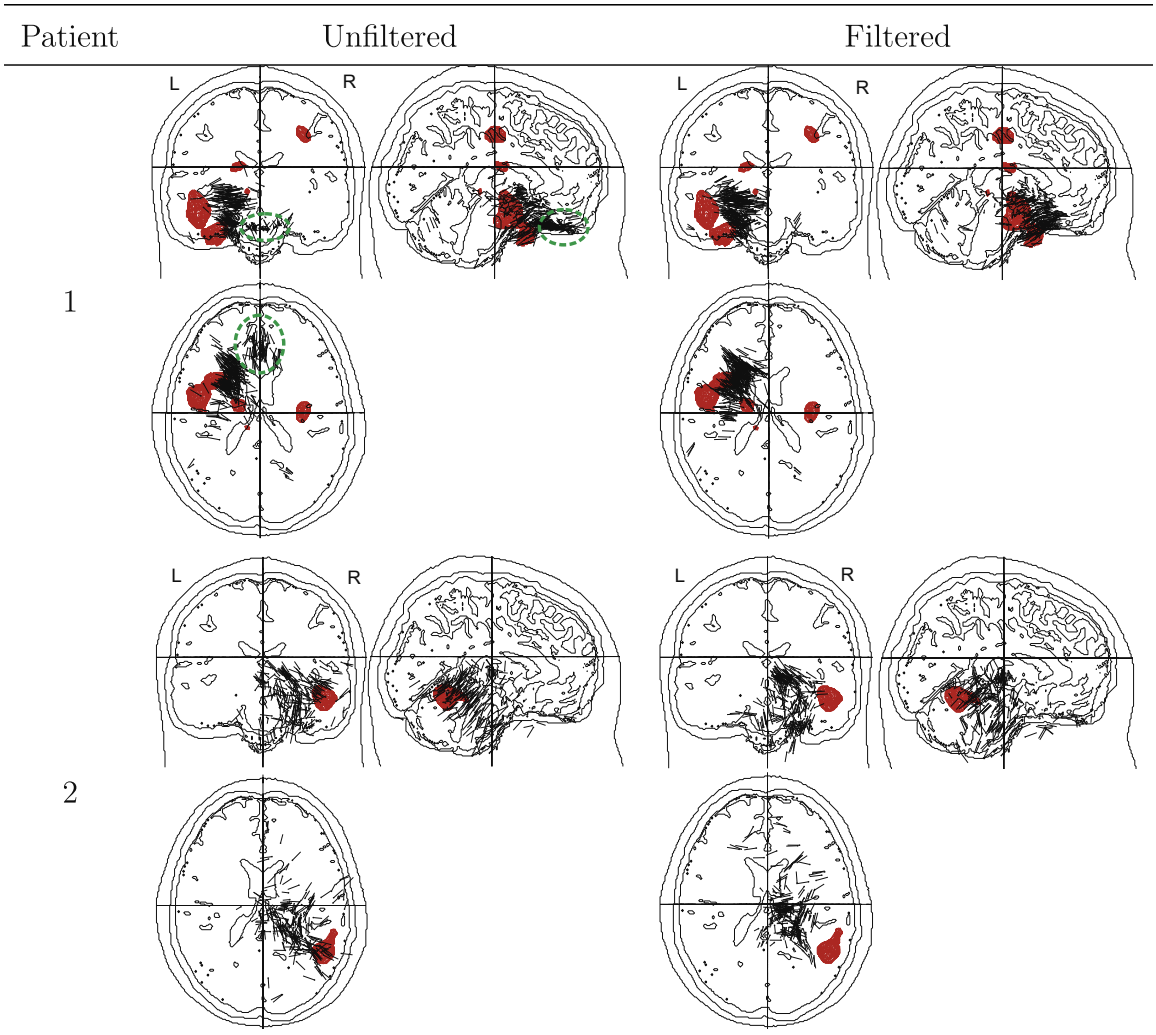


Fig. 4. Patients 1 and 2: The dipole estimations during a 21 s interval starting one second prior to the start of the seizure in the case of the unfiltered EEG data (left) and filtered EEG data (right). Each figure depicts three views of the dipole estimations in the realistic head model: axial, sagittal and coronal. The red contour denote the thresholded ictal SPECT activity coregistered with the realistic head model. For the sake of visualization, the threshold of the ictal SPECT was chosen to be 85% instead of the 95% used in the calculations (a 95% surface resulted in a very small area, which could be obscured by the dipole estimations). In patient 1 the green circle indicates a region of interest depicting the dipole estimations during an eye blink artifact. This results in dipole estimations estimated very near the eyes. (For interpretation of the references to color in this figure legend, the reader is referred to the web version of this paper.)

4. Results

4.1. Examples of artifact removal

In Figs. 2 and 3 examples are shown of the unfiltered and filtered EEG. Below each EEG segment, the distances of the dipoles to the thresholded ictal SPECT region is shown. An EEG segment contaminated with mainly muscle artifact is shown in Fig. 2a. The black asterisks and blue asterisks indicate the distance of the first and second dipole to the ictal SPECT activation, respectively. We can see that the distance has a high variability. Applying the muscle and eye artifact removal techniques results in the EEG shown in 2b. We can appreciate from the figures that the EEG muscle artifact has been reduced. As seen below the EEG segment, the distance measure is lower than in the one in the unfiltered EEG segment. The dipole estimates from this data set are shown in Fig. 5, patient 3.

To illustrate the filtering of eye blink artifacts, Fig. 3a and b show the EEG and the distance between the estimated dipoles and the edge of the ictal SPECT activation in the unfiltered and filtered case, respectively. While the ictal onset zone is located in the occipital area of the brain, the dipoles are located in the frontal area due to the eye blink artifacts (see Fig. 7, patient 8). When the eye blink artifacts are removed, the dipoles are located in the occipital area. In the vicinity of the start of the EEG seizure the dipoles were estimated within the enclosed surface of SPECT activity. This example shows that the filtering of the eye blink artifacts can improve the dipole estimation.

4.2. Estimation of the dipoles in the realistic head model

Figs. 4–7 show the dipole estimations during the 21 s interval (1 s prior to seizure onset till 20 s after) of the unfiltered EEG and filtered EEG for different patients. The red blob indicates the contours of the ictal SPECT activity. In the figures, regions of interest are marked in green or magenta. We will subdivide the results according to the improvement of the dipole estimations by applying muscle artifact removal and eye blink artifact removal. Finally, patients that did not show improvement are discussed.

The EEG segments of patients 3, 5 and 7 were mainly distorted by muscle artifacts. Therefore, dipole estimations are mainly seen in the bilateral temporal regions for patient 3 (Fig. 5) and patient 5 (Fig. 6) and in the parieto-occipital region caused by muscles in the neck in patient 7 (marked by the green ROI in Fig. 7). After artifact removal in patient 3 and 5 new clusters of dipoles emerged. In patient 3 (Fig. 5) the emerged dipole clusters show a good agreement with the ictal SPECT activity at the left temporal region. In patient 5 two very tight clusters appeared (marked by the magenta

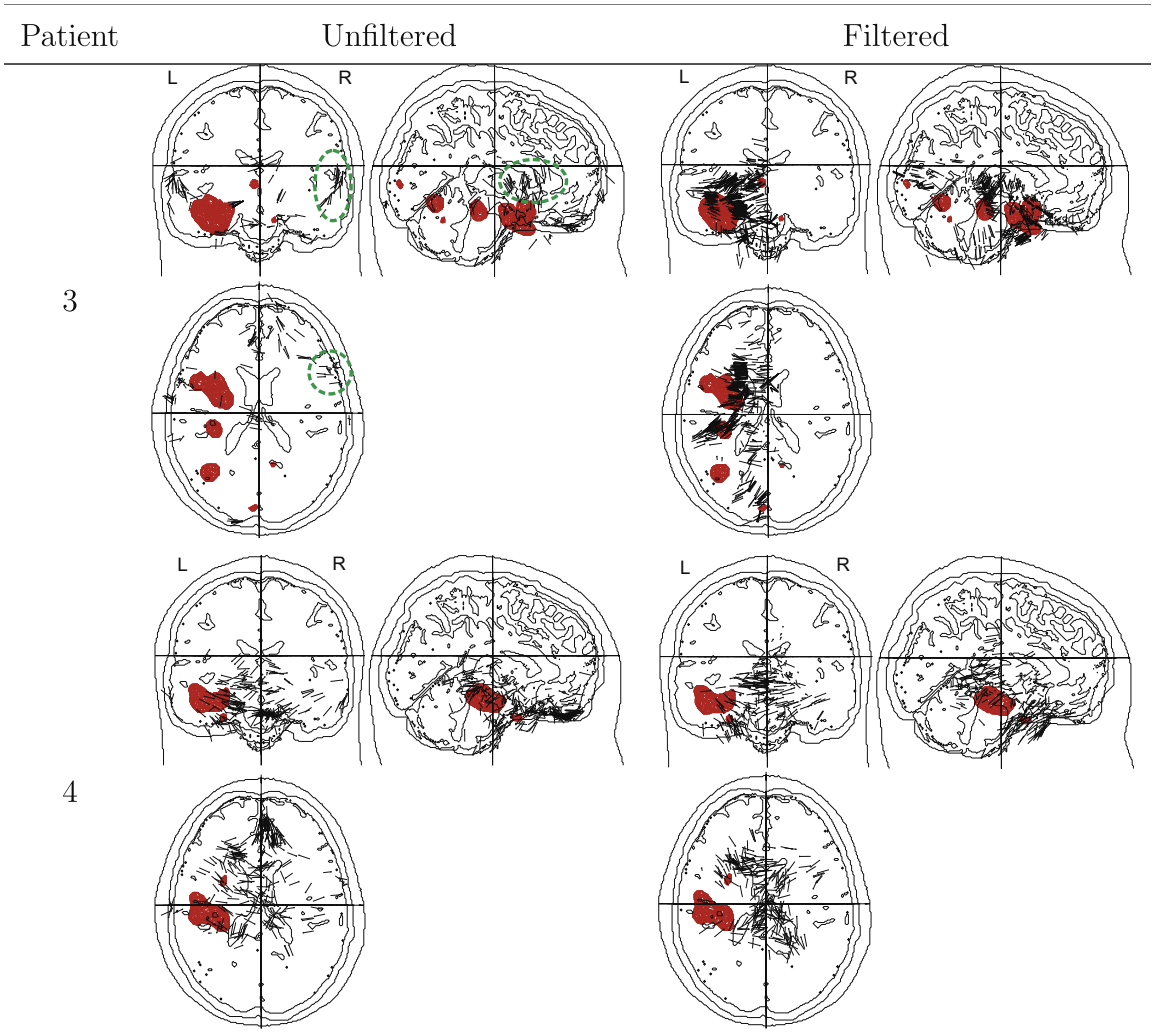


Fig. 5. Same as for Fig. 4, but for patients 3 and 4. In patient 3 the green circle indicates a region of interest depicting the dipole estimations due to the muscle activity. This results in dipole estimations estimated very near to the muscles. (For interpretation of the references to color in this figure legend, the reader is referred to the web version of this paper.)

ROIs) in Fig. 6. Although it is not clear from the figure, several dipole estimations had nearly the same location and orientation. After artifact removal in patient 7 (see Fig. 7), we see that the estimated dipole sources during the ictal episode are situated more frontally near the ictal SPECT regions.

The dipole estimation of patients 1 and 8 using the unfiltered EEG segments revealed many dipoles at the front of the head, marked by the green ROI in Fig. 4 (for patient 1) and Fig. 7 (for patient 8). These dipoles are caused by eye blink artifacts in the unfiltered EEG. After filtering, the activity in the front of the head of patient 1 and 8 was removed successfully. This resulted in more tight cluster in patient 1 in the left temporal lobe very close to the ictal SPECT activation. Patient 8 showed a significant improvement when the eye and muscle artifacts are removed. This resulted in a cluster in the parietal lobe which overlapped with the ictal SPECT.

Patients 2, 4 and 6 showed less or no improvement. Patient 6 (see Fig. 6) had an electrode artifact in the EEG. This is visible in the dipole estimations of the unfiltered data. After filtering, the electrode artifact is still present (indicated by the green ROI in both unfiltered and filtered dipole estimations). In the right parietal region, some muscle activity is present in the dipole estimation of the unfiltered EEG. Although after applying the muscle and eye blink artifact removal technique, the muscle activity was still present (marked by a magenta ROI). Patient 2 and 4 did not show a good agreement between the ictal SPECT and the dipole estimation after applying artifact removal. In the case of patient 2 (see Fig. 4) the ictal activity and the muscle activity contained the same spatial information. Thus removing the muscle activity, also removed components related to the ictal activity. Although in patient 4 (see Fig. 5) dipole estimations due to eye blink artifacts are successfully removed, the resulting dipole estimation after artifact removal are not near the ictal SPECT activation. A possible reason is that the epileptic activity cannot be modeled by the dipole model, as this kind of epileptic activity is not focal.

4.3. Comparing the distances

In Fig. 8 a boxcar plot of the distances between the dipole estimates to the ictal SPECT activations is shown for each patient in the unfiltered and filtered case.

5. Discussion

Ictal EEG is mostly contaminated with muscle and eye artifacts. This disturbs automatic source localization methods. We used

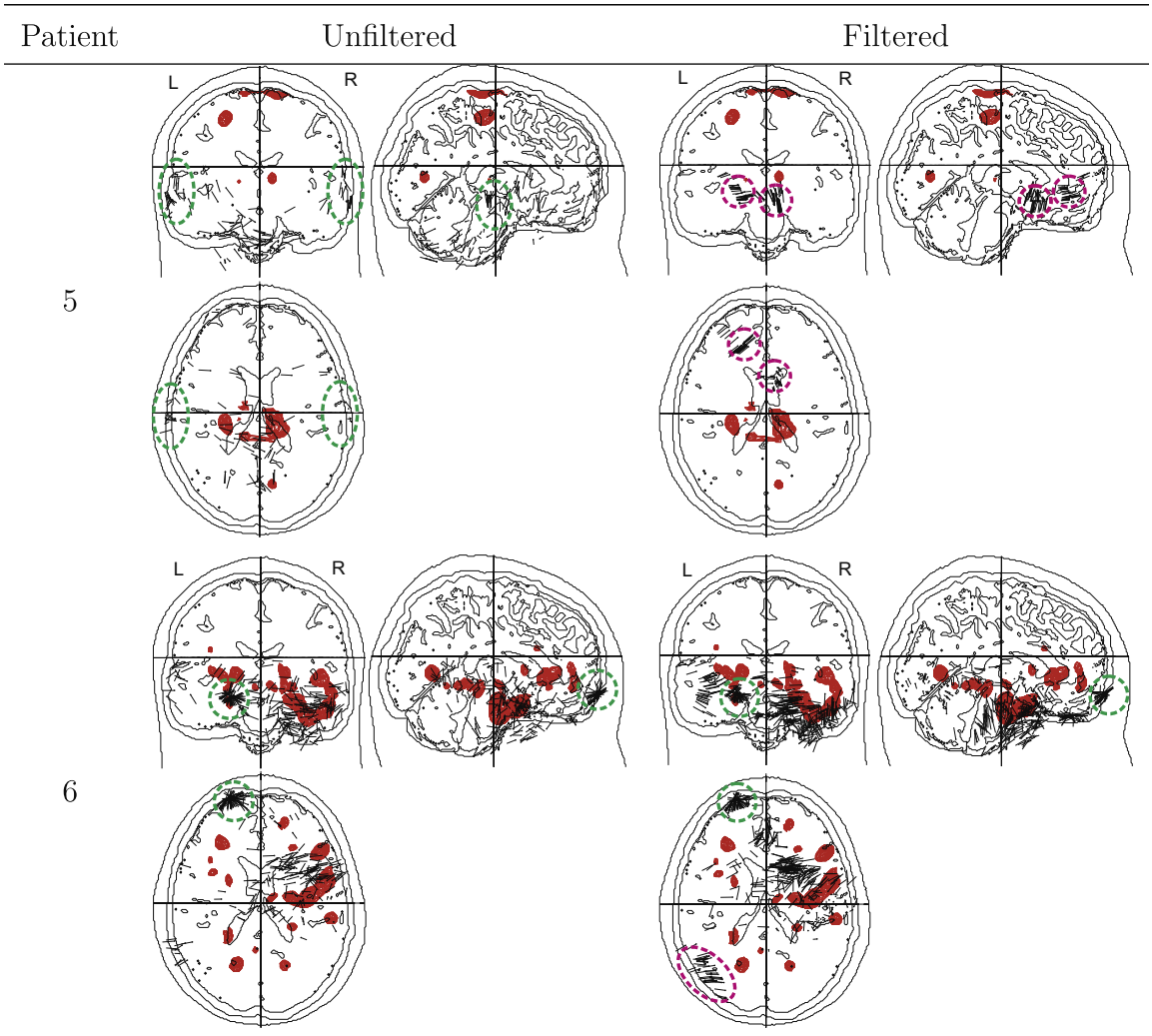


Fig. 6. Same as for Fig. 4, but for patients 5 and 6. In patient 5 the green circle indicates a region of interest depicting the dipole estimations due to the muscle activity. This results in dipole estimations estimated very near to muscle. The magenta circle in patient 5 indicates the two very tight clusters after artifact removal was applied. In patient 6 the green ROI indicates the dipoles due to the electrode artifact at one of the frontal electrodes. (For interpretation of color mentioned in this figure the reader is referred to the web version of the article.)

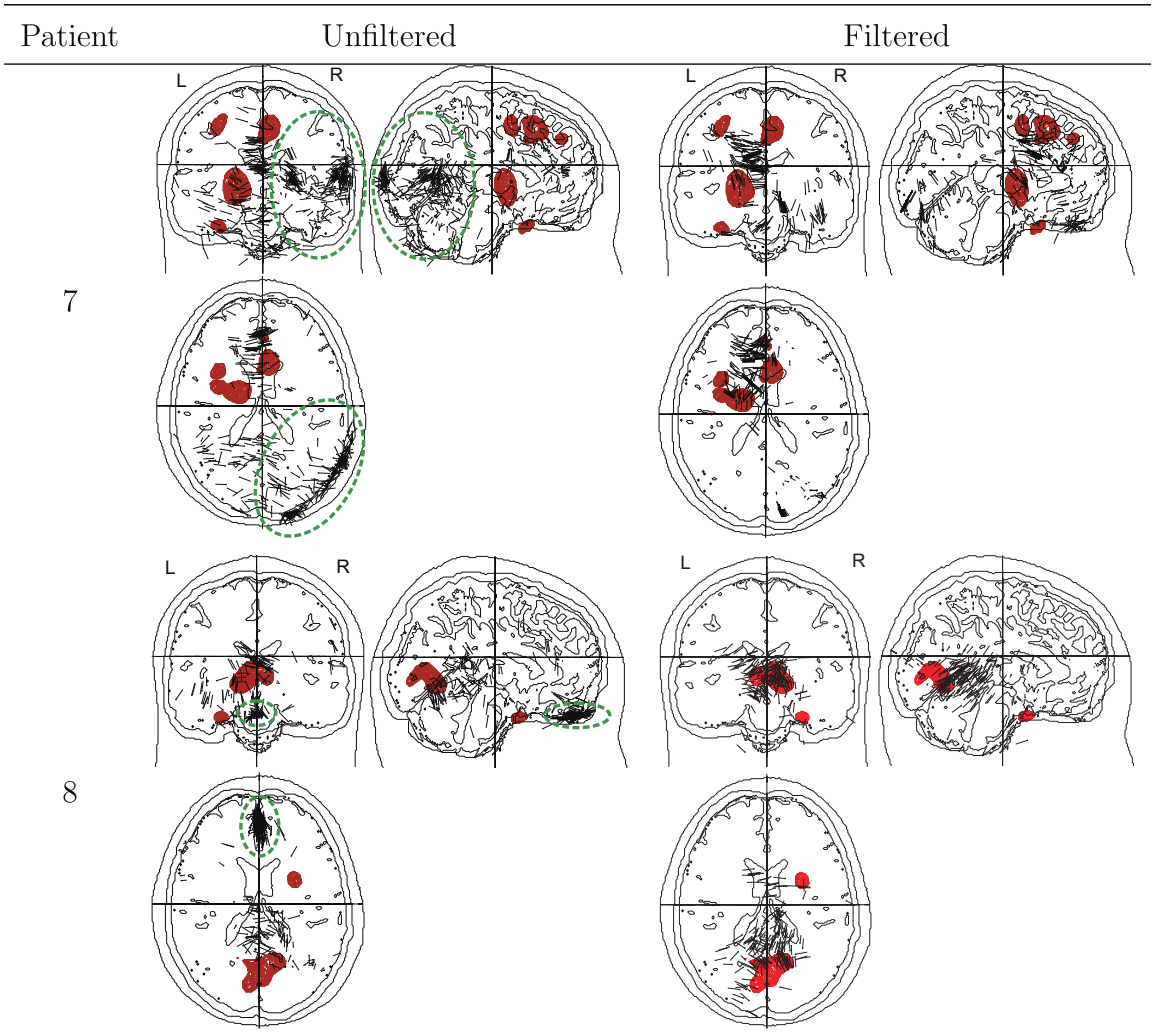


Fig. 7. Same as for Fig. 4, but for patients 7 and 8. In patient 7 the green circle indicates a region of interest which depicts the dipole estimation due to muscle activity. In patient 8 the green ROI depicts the dipoles during source analysis during eye blink artifacts. (For interpretation of color mentioned in this figure the reader is referred to the web version of the article.)

blind source separation techniques (BSS-CCA and SCICA) in order to remove these artifacts to obtain a better localization of the epileptogenic focus during ictal activity. In this small pilot study, we examined 8 patients suffering from epilepsy. To our knowledge we are the first who applied two artifact removal techniques prior to EEG dipole source localization. Most studies only consider the removal of eye blink artifacts (Nolte and Hämäläinen, 2001; Flanagan et al., 2002; Berg and Scherg, 1991) and only few studies report an improvement of the interpretation of the ictal EEG when muscle artifact removal is applied (Vergult et al., 2007). Furthermore the blind source separation technique, BSS-CCA, to remove muscle artifacts is a semi-automatic procedure, where the number components representing the muscle artifacts can be incremented or decremented by a button instead of visually inspecting and selecting the time series of the components if they contain muscle activity. The eye blink artifact removal technique is fully automatic. Regarding the RAP-MUSIC algorithm to estimate dipole sources, the separation between signal and noise subspace was different in the unfiltered and filtered EEG. After artifact removal the EEG consisted out of less components which had 95% of the explained variance in the EEG.

In this study the SPECT activation is used as an independent method to compare the source localizations with. However, ictal SPECT has a poor time resolution. Ictal SPECT hyperperfusion clusters, therefore, often display not only the ictal onset zone but also regions of ictal propagation (Van Paesschen et al., 2007). Ictal SPECT studies with early injection times, as in our study, are more likely to reflect the true ictal onset zone (Lee et al., 2006). Also, the ictal SPECT data, which are concordant with the other data of the presurgical evaluation, such as ictal semiology, interictal and ictal EEG and epileptic lesion on MRI, make it likely that the hyperperfusion cluster reflected the ictal onset zone, as in our patients. Also, four patients in the present study who underwent epilepsy surgery at the site of ictal SPECT hyperperfusion, obtained a good seizure outcome. We, therefore, believe that SISCOM in our carefully selected patients provided a valuable independent method to corroborate source solutions.

From Figs. 4, 5 and 7, we see clearly in patient 1, 3, 7 and 8 that removing the muscle and eye artifacts makes the dipole estimation more accurate. From Fig. 8 we see that the variability of the distance to the ictal SPECT activation decreases after filtering. However, in patient 8 the variability is low before filtering because of the dipole estimation in the frontal region due to the eye blink artifacts. Dipole clusters are more concentrated or new dipole clusters emerged near the ictal SPECT activations. This indicates a more reliable EEG source estimation when BSS-CCA and SCICA are

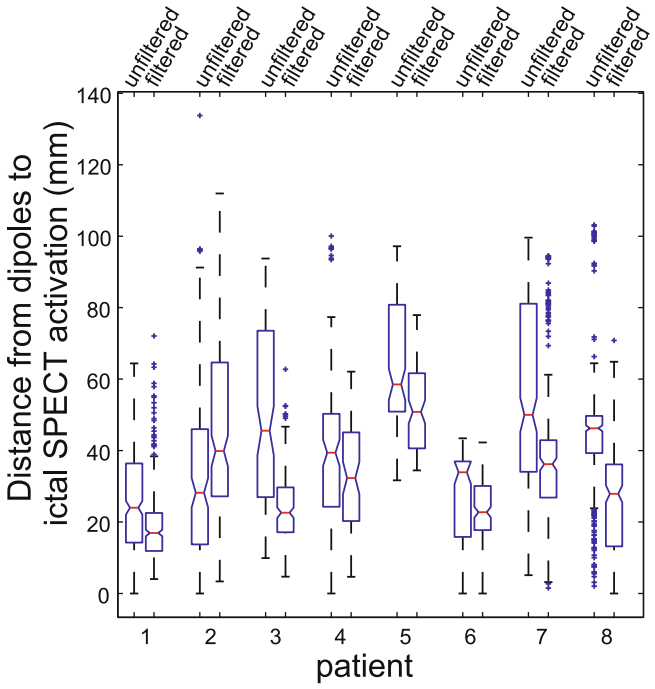


Fig. 8. A boxcar plot of the distance between the dipole locations and the edge of the ictal SPECT (iSPECT) activation for each patient.

applied. Patient 3 underwent a left anterior temporal lobe resection with the amygdala and hippocampus included. The patient has been seizure free (Engel I) since. The dipole estimation after the artifact removal were also situated in the left temporal lobe.

However, there are still some outliers and a perfect correlation between the dipole estimations and ictal SPECT is not obtained. This is due to the fact that source estimation depends on many parameters. One set of parameters is the head model. In the ideal case, the head model is a true representation of the head of the patient. In our study, the dataset did not contain individual MR images per patient. Thus a realistic head model from a standard T1 MR image was derived. Although the ictal SPECT can be coregistered with the MR image, the geometry of the head model plays an important role in the accuracy of the EEG source estimation. Moreover, the coregistration of the ictal SPECT image with an MR image, which did not originate from the patient, also introduces errors in the actual ictal SPECT location. Future studies will involve a more accurate and patient-specific description of the geometry of the head. This can be done by making head models from the MR images of individual patients, where fiducial markers at the electrodes can be used to extract the exact electrode positions.

In patient 2, 4 and 6 no improvement in the EEG source estimations were seen. This can also be deduced from the distance of the dipoles from the ictal SPECT in Fig. 8. The artifact removal in patient 5 improved the EEG source estimations and resulted in two very tight clusters. Careful examination of the unfiltered EEG during the ictal period showed excessive muscle activity. Therefore, the neurologist had to remove a lot of components in the BSS-CCA procedure until the ictal activity became visible. A singular value decomposition of the ictal EEG after filtering showed that the EEG can be described by only 3 or 4 components. In that case, the topographies in the SVD decomposition remain fixed for a period of 10 s. As the measurement space consists of 3 only components, the RAP-MUSIC algorithm resulted in very clustered dipole estimations. This resulted in dipole estimations with a high "goodness-of-fit" but with no physiological meaning as the ictal content of the signal was changed by the artifact removal techniques. Moreover, the muscle artifact removal was performed by the neurologist in 10 s windows. In each 10 s window components were removed until the neurologist was able to identify the EEG as muscle artifact free. However, the number of components removed differs from each 10 s window. This can result in abrupt changes of the signal-to-noise ratio at the 10 s window borders and thus in the dipole estimates location, which can be seen in Fig. 3. Future research will involve the automatic and more robust selection of components, so that the abrupt changes in the dipole estimates can be resolved and components related to muscle activity are better removed.

Patient 4, 5 and 6 underwent respective surgery. From patient 4 the left temporal lobe was resected which rendered the patient seizure free since 2003 (Engel I). Patient 5 received a focal resection of the left frontal focal cortical dysplasia and was rendered completely seizure free. Patient 6 underwent a resection of the temporal neocortex, inclusive of the amydala and the hippocampus. He was almost rendered seizure free (Engel II). In patient 4 and 5 no indication was given that the localization was improved. However, in patient 6 the dipole estimations before artifact removal already pointed in the right temporal neocortex, but no improvement was made by the muscle artifact removal techniques.

In Fig. 8 a boxcar plot of the distances to the edge of the ictal SPECT is depicted for each patient in the filtered and unfiltered case. The red line indicates the median. We clearly see that the dipole source estimation in patient 7 and 8 was improved by using the muscle and eye blink artifact removal. This is also clear from the dipole estimation in Fig. 7. The dipoles were estimated closer to the ictal SPECT activation. In patient 8 the median decreased, however the variability increased. This was due to dipole estimations of eye blink artifacts in the unfiltered EEG, which were positioned in the frontal region of the head. Furthermore, in patient 1 and 3 dipole estimations were located nearer the ictal SPECT activations after filtering.

To apply these techniques in the clinical practice, some work still has to be done. In the current paper the eye blink artefact removal was done automatically and the muscle artifact required little interaction of the clinician. The clinician applied the technique by means of a user interface to remove the muscle artifact and to determine the start of the seizure. Furthermore, a standard head model could be used to automatically coregister the SPECT data with and to perform the EEG source analysis. With an appropriate user interface, this can be done very quickly. However, if an individualized head model is used, one has to segment the MRI of the patient, determine the electrode positions and calculate the forward problem. The calculation of the forward problem can be done in an automatic way. However, the segmentation and the localization of the electrodes is tedious and requires the interaction of the clinician or nurse.

6. Conclusion

In 5 out of 8 patients an improvement of the EEG dipole estimation could be observed. In these patients tighter clusters or new clusters were observed near or overlapping with the ictal SPECT activity. This suggests that EEG source estimation can correctly depict the ictal onset zone if artifacts are removed.

However, some things are to be kept in mind. In EEGs moderately contaminated with muscle artifacts, however, BSS-CCA provides a more reliable estimation of the sources. In cases of severe muscle contamination of the EEG careful application of the BSS-CCA is advised. Moreover, when the muscle artifact had a different spatial information as the spatial information of the epileptiform

event, the expert did not remove many components using the BSS-CCA procedure.

The removal of eye artifacts using SCICA proved to be useful in EEG source estimation. The application of the artifact removal successfully eliminated the dipole estimates which corresponded to the eye artifacts. High resolution EEG may be useful in selected patients undergoing presurgical evaluation, and we predict that removing muscle artifacts, as described in the present paper, may lead to clinically relevant localizing data which could not be obtained in another way.

Finally, we want to state that this study is intended as a proof-of-principle exercise and not intended for routine practice. In routine practice, the clinical protocol should be extended by the adequate medical imaging techniques to construct an individualized head model for the EEG source analysis.

Acknowledgements

This work was supported by FWO project G.0360.05, IWT PhD grant (M. De Vos), GOA-AMBioRICS, IDO 05/010 EEG-fMRI, IUAP P6/04 DYSCO.

Appendix A. Supplementary data

Supplementary data associated with this article can be found, in the online version, at doi:10.1016/j.clinph.2009.05.010.

References

Assaf BA, Ebersole JS. Continuous source imaging of scalp ictal rhythms in temporal lobe epilepsy. Epilepsia 1997;38(10):1114–23.

Baillet S, Mosher JC, Leahy RM. Electromagnetic brain mapping. IEEE Signal Process Mag Nov 2001:14–30.

Belouchrani A, Abed-Meraim K, Cardoso J, Moulines E. A blind source separation technique using second-order statistics. IEEE Trans Signal Process 1997;45:434–44.

Belouchrani A, Abed-Meraim K, Hua Y. Jacobi-like algorithms for joint block diagonalization: applications to source localization. In: Proceedings of the IEEE int. workshop on intelligent signal processing and communication systems (ISPACS) CD-ROM.

Berg P, Scherg M. Dipole modelling of eye activity and its application to the removal of eye artefacts from the EEG and MEG. Clin Phys Physiol Meas 1991;12:49–54.

Boon P, D'Havé M, Vanrumste B, Hoey GV, Vonck K, Walleghem PV, et al. Ictal source localization in presurgical patients with refractory epilepsy. J Clin Neurophysiol 2002;19(5):461–8.

Comon P. Independent component analysis, a new concept? Signal Process 1994;36(3):287–314.

De Clercq W, Vergult A, Vanrumste B, Van Paesschen W, Van Huffel S. Canonical correlation analysis applied to remove muscle artifacts from the electroenceaphalogram. IEEE Trans Biomed Eng 2006;53(12):2583–7.

De Vos M. Spatially constrained independent component analysis and applications in neuroscience. Tech. Rep. 09-02. Leuven, Belgium: ESAT - SCD, KULeuven; 2009.

De Vos M, De Lathauwer L, Vergult A, De Clercq W, Van Paesschen W, Van Huffel S. Jacobi iterations for spatially constrained independent component analysis. In: Proc. of the 7th international conference on mathematics in signal processing (IMA 2007). England: Cirencester; 2006a

De Vos M, De Lathauwer L, Vergult A, De Clercq W, Van Paesschen W, Van Huffel S. Spatially constrained independent component analysis for real-time eye artifact removal from the electroencephalogram. In: Proc. of the first annual symposium of the IEEE/EMBS benelux chapter (IEEE EMBS); 2006b. p. 159–63.

Ding L, Worrell GA, Lagerlund TD, He B. 3D source localization of interictal spikes in epilepsy patients with MRI lesions. Phys Med Biol 2006;51(16):4047–62.

Flanagan D, Agarwal R, Wang Y, Gotman J. Improvement in the performance of automated spike detection using dipole source features for artefact rejection. Clin Neurophysiol 2002;114:38–49.

Friston KJ, editor. Statistical parametric mapping: the analysis of functional brain images. US: Academic Press Inc.; 2006.

Gonçalves S, de Munck J, Verbunt J, Bijma F, Heethaar R, Lopes da Silva F, et al. In vivo measurement of the brain and skull resistivities using an eit-based method and realistic models for the head. Biomed Eng, IEEE Trans 2003;50(6):754–67.

Goncharova II, McFarland DJ, Vaughan TM, Wolpaw JR. Emg contamination of eeg: spectral and topographical characteristics. Clin Neurophysiol 2003;114(9):1580–93.

Hallez H, De Vos M, Phlypo R, Vanrumste B, Van Hese P, D'Asseler Y, et al . Can dipole modelling be improved by removing muscular and ocular artifacts from ictal scalp EEG? In: Proceedings of the 3rd international IEEE EMBS conference on neural engineering; 2007. p. 252–55.

Hallez H, Vanrumste B, Van Hese P, D'Asseler Y, Lemahieu I, Van de Walle R. A finite difference method with reciprocity used to incorporate anisotropy in electroencephalogram dipole source localization. Phys Med Biol 2005;50:3787–806.

Hotelling H. Relations between two sets of variates. Biometrika 1936;28:321–77.

Jung TP, Makeig S, Humphries C, Lee TW, McKeown MJ, Iragui V, et al. Removing electroencephalographic artifacts by blind source separation. Psychophysiology 2000;37(2):163–78.

Lee S, Lee S, Yun C, Lee H, Lee J, Lee D. Ictal SPECT in neocortical epilepsies: clinical usefulness and factors affecting the pattern of hyperperfusion. Neuroradiology 2006;48:678–84.

Mosher JC, Leahy RM. Source localization using recursively applied and projected (RAP) MUSIC. IEEE Trans Signal Process 1999;47:332–40.

Niedermeyer E, Lopez Da Silva F. Electroencephalography: basic principles, clinical applications, and related fields. 5th ed. Lippincott: Williams & Wilkins; 2004.

Nolte G, Hämäläinen M. Partial signal space projection for artefact removal in MEG measurements: a theoretical analysis. Phys Med Biol 2001;46:2873–87.

O'Brien T, So E, Mullan B, Hauser M, Brinkmann B, Bohnen N, et al. Subtraction ictal SPECT co-registered to MRI improves clinical usefulness in localizing the surgical seizure focus. Neurology 1998;50:445–54.

Plummer C, Harvey SA, Cook M. EEG source localization in focal epilepsy: where are we now? Epilepsia 2008;49:201–18.

Shoker L, Sanei S, Wang W, Chambers JA. Removal of eye blinking artifact from the electro-encephalogram, incorporating a new constrained blind source separation algorithm. Med Biol Eng Comput 2005;43(2):290–5.

Van Paesschen W, Dupont P, Sunaert S, Goffin K, Van Laere K. The use of SPECT and PET in routine clinical practice in epilepsy. Curr Opin Neurol 2007;20:194–202.

Vergult A, De Clercq W, Palmini A, Vanrumste B, Dupont P, Van Huffel S, et al. Improving the interpretation of ictal scalp EEG: BSS-CCA algorithm for muscle artifact removal. Epilepsia 2007;48:950–8.